Macromolecular Reaction Engineering
www.mre-journal.de

An Integrated PRE Methodology for Capturing the Reaction Performance of Single- and Multi-site Type Catalysts Using Bench-Scale Polymerization Experiments

Vasileios Touloupidis, Gerold Rittenschober, and Christian Paulik*

The scope of polymer reaction engineering (PRE) is to develop a modeling pathway from polymerization process conditions to polymer microstructure and end-use properties. The catalyst is the heart of the low-pressure polymerization and its kinetic parameters constitute the cornerstone of this pathway, without which none of the modeling steps can be established. In this work, an integrated PRE methodology for capturing the reaction performance of single- and multi-site type catalysts is presented. According to the methodology proposed, the catalyst kinetic parameters are estimated based on a series of targeted bench-scale polymerization experiments and characterization combined with polymer reaction engineering modeling.

1. Introduction

Polyolefins have shaped the modern world over the last 70 years. The discovery of the Phillips catalysts in the early 1950s and the Ziegler–Natta catalysts some years later, enabled us to conduct ethylene and propylene polymerization under mild temperature and pressure conditions via an economically viable and safe process. Later, in the 1970s, the discovery of metallocene/methylaluminoxane (MAO) catalyst systems, facilitated the precise development of polyolefins with well-defined microstructure.[1] Since then, through continuous innovation in the field of catalysis and process technology, polyolefins managed to become the material of our era.

Nowadays, the world production of polyolefins exceeds 178 million tons.[2] The success of this class of materials lies on the wide range of properties that different polyolefin grades may exhibit as well as on the process flexibility and the degrees of freedom the modern polymerization technologies offer in order to properly tune their performance in a wide range of applications (from building and construction to automotive, packaging, and medical applications).

The humble polymer consisting of building blocks of ethylene, propylene and α-olefins is actually far from being simple, able to be formulated under infinite combinations of the inter- and intramolecular distributions that describe it.

Polymer reaction engineering (PRE) offers the theoretical background for describing the catalytic olefin polymerization process. The scope is to develop a modeling pathway from polymerization process conditions to polymer microstructure and end-use properties. This enables us not only to better understand the process but also to establish a mathematical tool for predicting the reactor and the polymer performance under different reaction conditions. This PRE pathway consists of concrete and well-defined steps (**Figure 1**):[3]

1. Connection of reaction conditions to polymer microstructure. This is the core component of PRE. The target is to translate the polymerization recipe (e.g., reactants' feeds, temperature, concentration) and the catalyst reaction performance to the expected polymerization rate and polymer molecular structure.
2. Connection of microstructure to first level properties. First level properties include all the polymer properties that are directly affected by polymer microstructure. A typical example would be the polymer density or melt viscosity that both come as a result of given polymer molecular weight distribution (MWD) and chemical composition distribution (CCD).
3. Connection of second level properties to the first level ones. The metaproperties that can be predicted as a function of microstructure and/or first level properties are defined as second-level properties. An example of a second level property would be melt index that is a result of the given melt viscosity for the shear rate range developed during flow under defined conditions.[4]

As it can be easily understood, the polymer microstructure acts as the common link between the reaction conditions and the polymer properties. Polyethylene microstructure refers to the MWD, CCD, or short-chain branching distribution (SCBD), comonomer sequence length distribution (CSLD), and long-chain branching distribution (LCBD). For the more complex case of polypropylene, microstructure also considers its regio- and stereochemical distributions. Nevertheless, the catalyst is the heart of the low-pressure polymerization process and its kinetic

Dr. V. Touloupidis
Modeling & Simulation Department
Borealis Polyolefine GmbH
St.-Peter-Straße 25
Linz 4021, Austria
E-mail: Vasileios.Touloupidis@borealisgroup.com
G. Rittenschober, Prof. C. Paulik
Institute for Chemical Technology of Organic Materials
Johannes Kepler University Linz
Altenberger Strasse 69, Linz 4040, Austria
The ORCID identification number(s) for the author(s) of this article can be found under https://doi.org/10.1002/mren.202000028.

DOI: 10.1002/mren.202000028

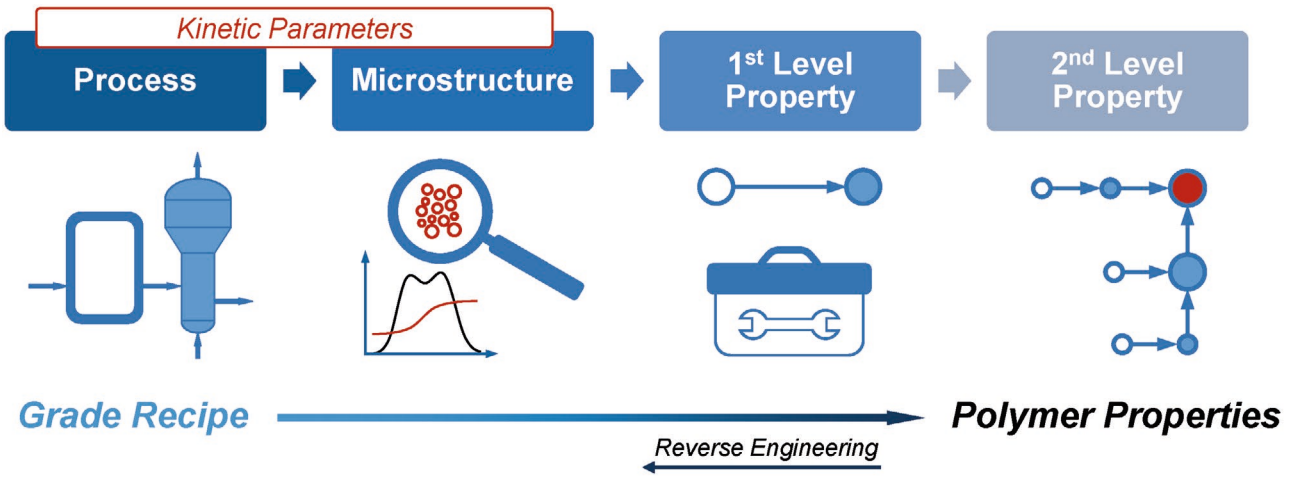

Figure 1. PRE pathway from polymerization recipe to properties.

parameters constitute the cornerstone of the PRE pathway, without which none of the modeling steps can be established.

In the age of the circular economy transformation of polymer business, the use of reaction engineering and process modeling tools for detailed process understanding, scale-up and intensification, becomes (more than ever) an indispensable component for the success of polymer business. This work focuses on the first modeling step of the integrated PRE methodology, establishing the connection of reaction conditions to polymer microstructure. More specifically, the PRE methodology for capturing the reaction performance of single- and multi-site type catalysts using bench-scale polymerization experiments is presented. According to the methodology proposed, i) the catalyst system is polymerized in bench-scale reactors in order to reveal the main responses, ii) the polymer is characterized via limited and targeted measurements, and iii) the PRE model provides us the catalyst kinetic parameters. These parameters, that remain constant, describe the catalyst reaction performance and they can then ensure an efficient scale-up and operation to pilot and commercial plants.

Over the last 25 years, Dr. João Soares has significantly contributed to the success of polymer business. His valuable ideas, process analysis studies and theoretical and applied solutions, presented in over 200 scientific publications and 14 books, developed and further expanded the polymer reaction engineering capabilities. This work is dedicated to Dr. João Soares, whose scientific contribution but also his integrity and contagious enthusiasm, motivates and inspires us the pursuit of PRE excellence.

2. Bench-Scale Polymerization

2.1. Reactor Setup

The polymerization experiments were carried out in a 5 L batch reactor (Büchi) constructed for a maximum pressure of 60 bar. A helical stirrer ensures good mixing conditions in slurry and in gas phase polymerizations. A jacket heating system is used for temperature control.

Ethylene and hydrogen can be introduced in the reactor either by batch-dosing or continuously with thermal mass flow controllers (MFCs). During polymerization experiments, ethylene is continuously fed in order to maintain the pressure at the desired set-point, counterbalancing the pressure decrease due to monomer consumption. In order to increase the feeding accuracy, two ethylene MFCs are employed, providing higher dosing accuracy depending on the feed rate (5 or 25 g min^{-1} maximum mass flow). The monomer inflow rate can be used for precise monitoring of the polymerization activity. The comonomer (in this instance 1-butene) can be added to the reactor with a syringe pump (Teledyne ISCO).

The Ziegler–Natta catalyst suspension, triethylaluminum (TEA) and triisobutylaluminum (TIBA) are prepared offline in a glovebox and they are then transferred into the reactor by an injection unit consisting of a pneumatically driven cylinder. The resulting pressure spikes are minor and stable process conditions are reached shortly after the injection. The temperature, reactor pressure and mass flow values are being continuously recorded during the experiment by a data acquisition/control unit (3852A, HP) connected to a program written in Agilent VEE (which also manipulates the MFCs).

2.2. Chemicals

The polymerization experiments were carried out with an industrial Ziegler–Natta catalyst provided as a suspension in mineral oil. Triethylaluminum (93%, Sigma-Aldrich) was used as cocatalyst and triisobutylaluminum (Sigma-Aldrich) acted as scavenger of catalyst poisons during the experiment preparations. All the chemicals mentioned below underwent purification in a setup consisting of copper catalysts and molsieves.[5] *n*-Heptane (≥99%, Roth) was used as diluent for catalyst injection. The reactor was purged with nitrogen (5.0, Linde) during preparations. The reaction medium for slurry phase polymerization was propane (3.5, Gerling Holz & Co.). Furthermore, ethylene (3.0, Linde), hydrogen (5.0, Linde), and optionally 1-butene (2.5, Linde) were fed into the reactor.

2.3. Polymerization Procedure

Before starting a polymerization experiment, the reactor undergoes a cleaning process. The reactor is heated up to 95 °C and approximately 40 mg of TIBA is injected into the reactor to scavenge impurities. Afterward, an automated purge program is started. The hydrogen and ethylene MFCs are purged and the reactor is pressurized with nitrogen to 5 bar and evacuated subsequently. This step is repeated three times. Residual amounts of nitrogen are removed by purging with propane.

The reactor is filled with 1 kg of propane, and the cocatalyst (triethylaluminum) is injected. The reactor is heated up to prepolymerization temperature. At the same time, hydrogen and ethylene are added via the MFCs. The reaction starts by injecting the Ziegler–Natta catalyst suspension. A prepolymerization step is included in order to properly condition the catalyst at lower temperature before introducing it to the actual reaction conditions, avoiding fragmentation issues. After the desired prepolymerization time (typically up to 10 min), the reactor is heated up to the actual slurry phase polymerization temperature. This transition time should remain as short as possible since polymerization continues to take place producing an intermediate product (for our setup: 10 min). During the heating phase, additional amounts of hydrogen and comonomer are fed into the reactor. Afterward, the ethylene is added in order to reach the pressure set point at the respective reaction temperature (for our setup, the pressure set point is set at 50 bar). According to the control scheme, ethylene is continuously added during polymerization to keep the pressure constant and its uptake is continuously monitored. The slurry phase polymerization continues for the selected reaction time and it is terminated by opening the outlet valve. The pressure decrease leads to the gasification and removal of all non-solid components (i.e., propane, ethylene, hydrogen) leaving in the reactor the solid product (i.e., polymer, embedded catalyst, and sorbed reactants). In case of a multistage polymerization, (e.g., slurry or gas phase polymerization) the reactor temperature is properly adjusted and hydrogen, ethylene, and comonomer are fed in order to reach the desired concentrations. Once again, the transition time should be minimized according to the setup capabilities (for our setup, 20 min are required for the slurry-gas transition). After the polymerization is complete, the outlet valve is opened. If no further gas phase polymerization is to be carried out, the reactor is then purged with nitrogen and opened to obtain the synthesized polymer. The polymer is dried overnight at 70 °C in a vacuum oven in order to remove most of the sorbed component (degassing). The reactor itself is cleaned, closed, evacuated, and purged with nitrogen several times.

2.4. Polymer Characterization: Size Exclusion Chromatography

Analyzing the obtained polymers by high-temperature size exclusion chromatography (HT-SEC) reveals the molecular mass distribution and frequency of short chain branching. The device used was a GPC-IR (Polymer Char) equipped with an IR5 detector and three PLgel Olexis columns (300 × 7.5 mm, Agilent). The eluent was 1,2,4-trichlorobenzene, the samples were dissolved at 160 °C for 120 min.

3. Polymer Reaction Engineering

In what follows, an integrated PRE methodology for capturing the main apparent kinetic parameters of single- and multi-site type catalysts using bench-scale polymerization is presented. This is the first step toward the detailed estimation of the catalyst kinetic parameters that describe its reaction performance and forms the basis for any further more advanced PRE efforts. The model development begins with the simplest approach possible. If this is not enough in order to explain the experimental reaction performance acquired, the model is extended accordingly. This way, the model detail always remains on the level of what can be observed and measured.

3.1. A Unified Approach for Single- and Multi-site Catalysts

Multi-site catalysts are considered to be a mixture of single-site catalysts, referring to different site types. This assumption is able to describe the distinctive features of a multi-site catalyst, including a broader MWD and a distribution of comonomer content (CC) along the MWD, contrary to the narrower MWD (polydispersity = 2) and constant CC along MWD corresponding to the use of a single-site catalyst (for steady-state conditions). The initial fraction of its single-site catalyst components (or site types) is a characteristic property of the given multi-site catalyst and remains constant. Each site type exhibits its own reaction performance in terms of reactivity and responses (e.g., hydrogen effect or comonomer incorporation) and can be described by its own set of kinetic parameters. When all site types share the same kinetic parameter values for activation, propagation, and deactivation, the weight fraction of the polymer produced by these site types remains the same as their initial distribution during polymerization. In case any of these kinetic parameters differs, the site type weight fraction will be affected accordingly. For example, if a site type deactivates faster than the others, the weight fraction of the polymer produced by this site type will dynamically decrease in time (starting from the site type fraction value) in contrast to the corresponding increase of the remaining site types.

The MWD of a multi-site catalyst n_s site types, D_{ms}, can be described as[6,7]

$$D_{ms} = \sum_{i}^{n_s} w_i D_{ss,i} \tag{1}$$

where $D_{ss,i}$ is the MWD of its single-site components and w_i is the corresponding weight fraction of the polymer produced by each site type. The single-site catalyst MWD is described by the Schulz–Flory one-parameter distribution (where r corresponds to the degree of polymerization), always leading to a polydispersity value of 2:[8]

$$D_{ss,i}(r) = r\left(\tau^i\right)^2 e^{-r\tau^i} \tag{2}$$

The distribution parameter, τ^i, defines the peak of the site type MWD and it is equal to the inverse of the number average degree of polymerization, DP_n^i:

$$\tau^i = \frac{1}{DP_n^i} = \frac{\overline{MW}}{M_n^i} = \frac{2\,\overline{MW}}{M_w^i} \tag{3}$$

where M_n^i and M_w^i refer to the number- and weight-average molecular weight and $\overline{MW}$ is the molecular weight of the repeating unit (e.g., for polyethylene, $\overline{MW} = 28.05$ g mol^{-1}).

Following the same approach, the comonomer composition along the molecular weight of a multi-site type catalyst, C_{ms}, results as the weighted sum of its single-site components:

$$C_{ms} = \frac{1}{D_{ms}} \sum_i^{n_s} w_i D_{ss,i} \overline{F_{B,i}} \tag{4}$$

where $\overline{F_{B,i}}$ refers to the average comonomer composition of each site type present.

3.2. Apparent Activation, Propagation, and Deactivation

According to the simplest kinetic scheme that can describe the catalytic polymerization rate, the initial catalyst, C, needs to be activated to a "live" polymer chain of zero chain length, P_0. "Live" polymer chains of chain length r, react with the monomer, A, adding one more building block until they deactivate, leading to a "dead" polymer chain, D_r, and the deactivated catalyst, C_d:

$$C \xrightarrow{ka} P_0 \tag{5}$$

$$P_r + A \xrightarrow{kp} P_{r+1} \tag{6}$$

$$P_r \xrightarrow{kd} D_r + C_d \tag{7}$$

The first step toward the description of the catalyst reaction performance is the estimation of the apparent activation, k_a, propagation, k_p, and deactivation, k_d, parameters. The kinetic mechanism may actually comprise a more complex set of elementary reactions.[9] At this stage however, the absolute value of each parameter (for a given temperature) is estimated irrespective of the possible underlying kinetic mechanisms.

The polymerization rate, R_p, the rate of production/consumption of the living chains, $\frac{d[Y]}{dt}$, and the rate of consumption of catalyst, $\frac{d[C]}{dt}$, can be described by the following expressions:[6,10–12]

$$R_p = k_p [M][Y] \tag{8}$$

$$\frac{d[Y]}{dt} = k_a [C] - k_d [Y] \tag{9}$$

$$\frac{d[C]}{dt} = -k_a [C] \Rightarrow [C] = [C]_0 \exp(-k_a t) \tag{10}$$

Assuming that polymerization takes place in steady state, the above expressions can be integrated to the following expression for the rate of polymerization:

$$R_p = k_p [M][C]_0 \frac{\left\{1 - \exp\left[-k_a \left(1 - \left(k_d / k_a\right)\right) t\right]\right\} \exp(-k_d t)}{1 - \left(k_d / k_a\right)} \tag{11}$$

In this expression, the constant monomer concentration, $[M]$ (referring to the cumulative concentration of monomer, A, and comonomer, B, if present, $[M] = [A] + [B]$), as well as the initial catalyst concentration, $[C]_0$, is known. This way, the apparent kinetic parameters of activation, propagation, and deactivation can be directly estimated by fitting the experimentally measured polymerization rate. It should be noted that the monomer concentration should be either measured (e.g., using online IR detector for gas phase polymerization) or calculated based on thermodynamic modeling (considering the equilibrium concentration in the phase of interest). In this work, Sanchez–Lacombe equation of state was employed for the calculation of phase separation and the corresponding species concentrations in each phase present.

When a second monomer is present, the apparent kinetic parameter is calculated as[6]

$$k_p = \sum_i^{n_s} w_i \overline{k}_p^i = \sum_i^{n_s} w_i \left(k_{p,AA}^i \Phi_A^i f_A + k_{p,AB}^i \Phi_A^i f_B + k_{p,BA}^i \Phi_B^i f_A + k_{p,BB}^i \Phi_B^i f_B\right) \tag{12}$$

$$f_A = \frac{[A]}{[A]+[B]} \tag{13}$$

$$f_B = 1 - f_A \tag{14}$$

$$\Phi_A = \frac{k_{p.BA} f_A}{k_{p.BA} f_A + k_{p.AB}(1 - f_A)} \tag{15}$$

$$\Phi_B = 1 - \Phi_A \tag{16}$$

where $k_{p,xy}^i$ (according to the terminal model) refers to the kinetic parameter for an addition of y monomer to a chain ending in x monomer. These binary kinetic parameters are then directly connected to the comonomer content of the polymer produced per site type. If we have access to this information, the following expression regarding the comonomer content per site type, CC^i, should be fulfilled:

$$CC^i = \frac{k_{p,AB}^i \Phi_A^i f_B + k_{p,BB}^i \Phi_B^i f_B}{k_{p,AA}^i \Phi_A^i f_A + k_{p,AB}^i \Phi_A^i f_B + k_{p,BA}^i \Phi_B^i f_A + k_{p,BB}^i \Phi_B^i f_B} \tag{17}$$

As soon as we estimate the apparent propagation kinetic parameter and we have access to the MWD of the polymer produced per site type i (what is actually needed is the average molecular weight value), the apparent transfer parameter can be calculated. The distribution parameter, τ^i, is equal to the ratio of the transfer rate to the propagation rate, leading to the expression[13]

$$\tau^i = \frac{1}{DP_n^i} = \frac{\overline{MW}}{M_n^i} = \frac{2\,\overline{MW}}{M_w^i} = \frac{\text{transfer rate}}{\text{propagation rate}} = \frac{k_t^i}{k_p^i[A]} \Rightarrow k_t^i = \frac{2\,\overline{MW}}{M_w^i} k_p^i[A] \tag{18}$$

This apparent transfer parameter can then be split into different possible transfer mechanisms, including transfer to cocatalyst, to hydrogen or spontaneous transfer as

$$k_t^i = k_{t,T}^i[T] + k_{t,H}^i[H] + \cdots + k_{t,sp}^i \tag{19}$$

It is noted that this is a direct calculation for single-site catalysts, while for multi-site catalysts a deconvolution step is needed in advance in order to reveal the exact position of the MWD of each site type.

Since each catalyst system reacts in its own distinctive way, we can only identify these underlying mechanisms if we experience different chain transfer behavior when varying the affecting factors. Typically, since it is well known that hydrogen acts as a chain transfer agent for polyolefin polymerization and spontaneous transfer due to β-hydride-elimination is always present, these are the sine qua non components. For the case that only these two mechanisms are present, we should be able to experimentally witness it as a linear correlation between hydrogen concentration and apparent transfer parameter.

The same approach is also followed for revealing additional underlying kinetic mechanisms for activation and deactivation. Moreover, in rare cases where a catalyst reaction performance cannot be described by the existing mechanism, new elementary reactions might be needed to be included (e.g., catalyst site type transformation).

Finally, it is noted that all the kinetic parameters presented are affected by temperature, following the Arrhenius law:

$$k = Ke^{-E/RT} \tag{20}$$

This way, having estimated the kinetic parameter value for two different temperatures, the corresponding kinetic rate constant, K, and the constant pre-exponential parameter, E can be further calculated.

3.3. Distribution Split and Deconvolution

When polymerization process takes place in a continuous reactor series or a multistage polymerization in batch mode, it is only the microstructure of the resulting polymer at the end of the process that can be characterized. This microstructure actually refers to the cumulative sum of the microstructure of the polymer produced in each different reactor or stage of the process. The final MWD, D_f, and comonomer content, C_f, for a series of n_r reactors (or stages) are calculated as the weighted sum, based on the split value (the weight fraction of the polymer produced per reactor or stage), s_i, of all contributing distributions, D_i and C_i:

$$D_f = \sum_i^{n_r} s_i D_i \tag{21}$$

$$C_f = \frac{1}{D_f} \sum_i^{n_r} s_i D_i C_i \tag{22}$$

$$s_i = \frac{Y_i}{\sum_i^{n_r} Y_i} \tag{23}$$

In order to properly reveal the microstructure referring to each reactor or stage, a polymer sample has to be collected at the exit of each reactor for continuous processes, and, the process needs to stop at the end of each stage for batch processes. In both cases, however, the last reactor or stage will always refer to the sum of the microstructure entering the reactor or stage and the fresh polymer microstructure produced. In order to reveal this last reactor microstructure, a split calculation needs to be applied. For example, for a series of two reactors (in steady state) or two-stage polymerization, the calculation of the MWD of the final polymer, D_f, as well as the comonomer distribution is calculated as

$$D_2 = \frac{1}{s_2}(D_f - s_1 D_1) \tag{24}$$

$$C_2 = \frac{1}{s_2 D_2}(D_f C_f - s_1 D_1 C_1) \tag{25}$$

For the case of single-site catalysts, the application of the described PRE framework would be sufficient for a basic kinetic parameter estimation procedure. For the case of multi-site catalysts, the additional step of deconvolution to site types is required in order to gain access to the site type kinetic parameter values. This optimization procedure provides i) the minimum number of site types required in order to adequately reconstruct the experimental microstructure information, and, ii) a detailed estimation of site type weight fraction and microstructure. The process may be based on MWD, CCD, or even nuclear magnetic resonance spectroscopy information either separately or in combination. Many workers on the field have developed and applied deconvolution techniques.[14–16] In its simplest form, deconvolution refers only to MWD. In this case, the minimization target is the difference between the reconstructed MWD points, D_{ms}^k, and the experimentally measured points via HT-SEC, D_{exp}^k, for a given number of site types:

$$x^2 = \sum_k^{n_p} \left(D_{exp}^k - D_{ms}^k\right)^2 = \sum_k^{n_p} \left(D_{exp}^k - \sum_i^{n_s} w_i D_{ss,i}^k\right)^2 \tag{26}$$

under the constraint that

$$\sum_i^{n_s} w_i = 1 \tag{27}$$

As it can be understood, increasing the number of site types leads to higher reconstruction accuracy and at the same time

increased complexity for estimating the corresponding kinetic parameters. Typically, the reconstruction accuracy should lie below the sum of the experimental error and should be compromised at this level. Deconvolution is typically a loop process of trial and error; whenever new experimental measurements imply an error in the deconvolution estimation, the whole process should be revised. Moreover, whenever experimental evidence for the contrary are not present, the initial site type distribution should remain constant. The MWD deconvolution provides the final missing piece for estimating the transfer parameter per site type according to Equations (18) and (19).

The deconvolution process may continue to comonomer composition. After having estimated the number and position of the single-site distributions, the corresponding site type comonomer content can be estimated. In this case, the objective function becomes

$$x^2 = \sum_{k}^{n_p} \left(C_{exp}^{k} - C_{ms}^{k} \right)^2 = \sum_{k}^{n_p} \left(C_{exp}^{k} - \frac{1}{D_{ms}^{k}} \sum_{i}^{n_s} w_i D_{ss,i}^{k} C_{ss,i} \right)^2 \quad (28)$$

While both steps can be merged within the same optimization procedure, it is selected to proceed stepwise.[6] This way, the complexity is reduced and the comonomer content deconvolution becomes a test for the estimated weight fractions and positions. In case no consistent solution can be estimated, the MWD deconvolution has to be revised. The comonomer content deconvolution is then able to provide the basis for expanding the propagation parameter to its components according to Equations (12)–(17).

Finally, it is noted that the deconvolution process can be further expanded to more complex microstructural characteristics such as the CCD as well as the CSLD but this analysis is beyond the scope of this work.[6,17–20]

4. Results and Discussion

The scope of this work is to present an integrated PRE methodology for capturing single- and multi-site type catalysts reaction performance using bench-scale polymerization experiments. Since different catalyst systems may exhibit different reaction performance and consequently be described by a different set of kinetic parameters, the results section focuses on the parameter estimation methodology rather than on providing a full kinetic parameter set for the catalyst in use.

4.1. Polymerization Experiments

In order to reveal the main responses of the catalyst system and demonstrate the PRE methodology for estimating the corresponding kinetic parameters we proceeded to a total of 12 polymerization experiments (runs). The experimental plan is shown in **Table 1**. The runs 1–5 focus on the hydrogen response in slurry phase at 85 °C. The polymerization time for run 1 was extended to 120 min in order to have a more complete view of the catalyst profile including its deactivation behavior. For runs 2–5 the polymerization time was kept equal to 30 min. Accordingly, the runs 6–9 focus on the hydrogen response in slurry phase at 95 °C. The runs 10–12 introduce a second polymerization stage in gas phase and focus on the comonomer response.

4.2. Polymer Reaction Engineering: Activity Profiles

The apparent kinetic parameters for activation, propagation, and deactivation for slurry phase homopolymerization at 85 °C are estimated based on the corresponding activity profile (Run 1) via Equation (11). The experimental and modeling activity profiles are presented in **Figure 2**. The same apparent kinetic parameters are then used for the hydrogen response polymerization experiments (runs 2–5). The model is able to follow the experimentally measured activity profiles (**Figure 3**). As can be seen in Figure 3, there is an apparent effect of the hydrogen feed on the polymerization rate as the rate decreases for higher hydrogen feed. However, this is a result of the design of the bench-scale experiment: since the pressure setpoint is the same in all slurry phase experiments, an increase

Table 1. Experimental plan of polymerization experiments.

Run	Slurry phase				Gas phase			
	Temperature [°C]	H_2 [g]	C4 [g]	Time [min]	Temperature [°C]	H_2 [g]	C4 [g]	Time [min]
1	85	1.25	–	120	–	–	–	–
2	85	0.25	–	30	–	–	–	–
3	85	0.75	–	30	–	–	–	–
4	85	1.0	–	30	–	–	–	–
5	85	1.25	–	30	–	–	–	–
6	95	1.25	–	120	–	–	–	–
7	95	1.0	–	30	–	–	–	–
8	95	1.25	–	30	–	–	–	–
9	95	1.5	–	30	–	–	–	–
10	95	1.0	–	30	85	0.1	0	45
11	95	1.0	–	30	85	0.1	1	45
12	95	1.0	–	30	85	0.1	5	45

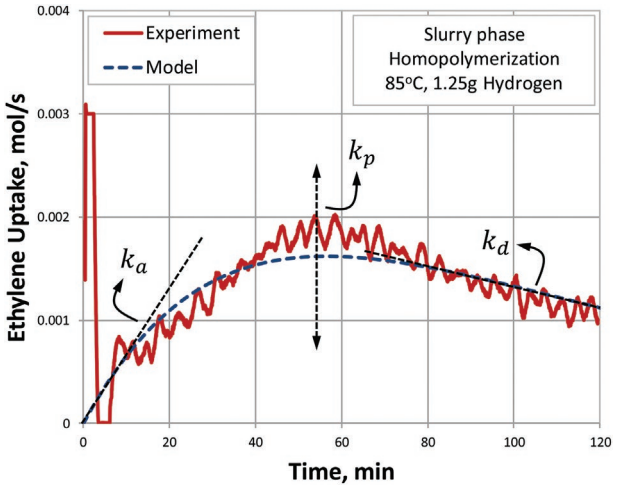

Figure 2. Activity profile for slurry phase homopolymerization at 85 °C (run 1).

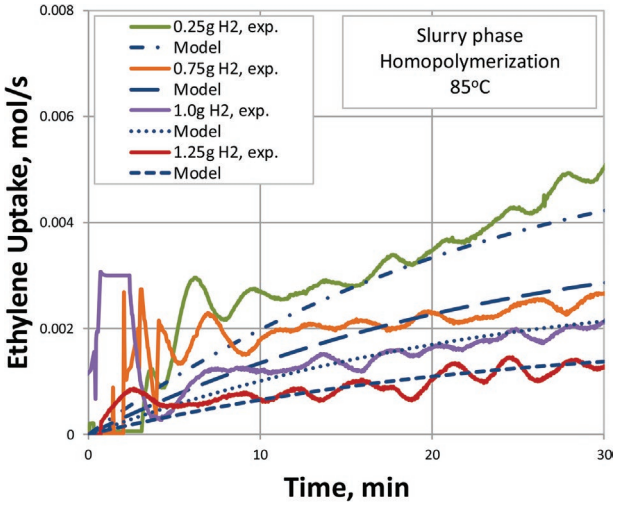

Figure 3. The effect of hydrogen on the activity profile for slurry phase homopolymerization at 85 °C (runs 2–5).

in hydrogen amount (via the batch-dosing), will reduce the need of ethylene feed in order to reach the desired pressure, leading to lower monomer concentrations and consequently lower polymerization rate. Thus, as these concentration values are considered by the model and the same kinetic parameters can explain the activity profiles for the hydrogen response runs, no additional hydrogen effect on propagation rate can be identified. This is an answer, a proper PRE analysis can provide, distinguishing the actual phenomena from the phenomenological observations.

In order to reveal the effect of temperature on the catalyst reaction performance, the hydrogen response runs were further conducted at 95 °C. The activity profile (run 6) as well as the effect of hydrogen (runs 7–9) on the activity profile for slurry phase homopolymerization at 95 °C are presented in **Figure 4**. The estimated apparent kinetic parameter values for slurry phase homopolymerization in 85 and 95 °C are gathered in **Table 2**. The Arrhenius law (Equation (20)) or similar correlation can be further used in order to consider the temperature effect on the kinetic parameter values.

4.3. Polymer Reaction Engineering: Polymer MWD

As discussed, the hydrogen feed (and consequent concentration) does not affect the polymerization rate (for this case). However, hydrogen acting as a chain transfer agent has a significant effect on the MWD of the polymer produced. This effect is clearly shown in **Figure 5**, where the additional hydrogen batch-feed leads to a shift of the MWD to lower chain length.

For single-site catalysts, the average molecular weight of the polymer produced combined with the estimated apparent propagation kinetic parameter would be enough in order to estimate

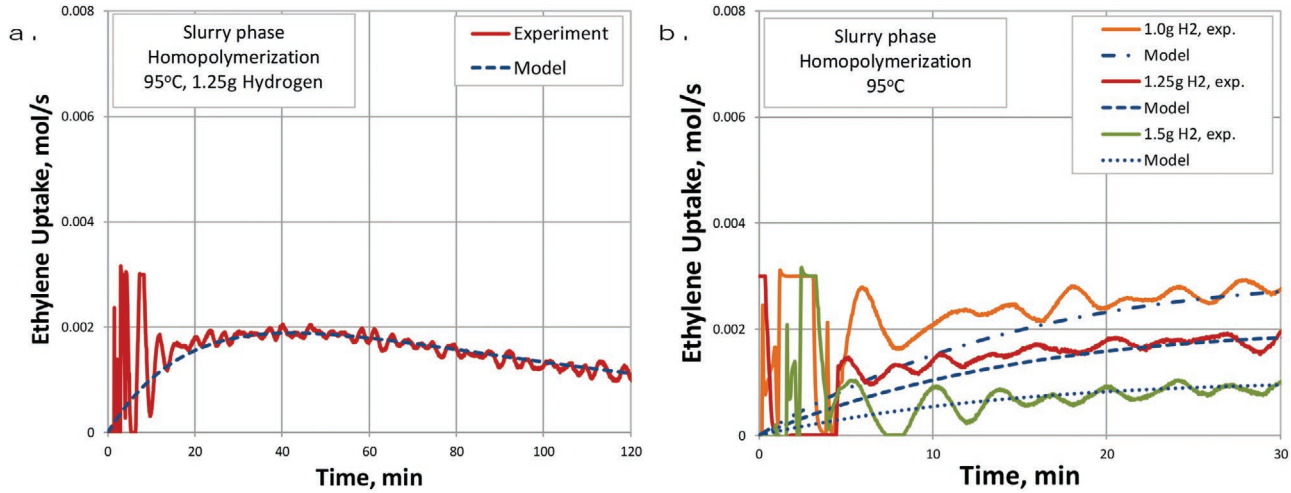

Figure 4. a) Activity profile for slurry phase homopolymerization at 95 °C (run 6) and b) the effect of hydrogen on the activity profile for slurry phase homopolymerization at 95 °C (runs 7–9).

Table 2. Apparent kinetic parameter values for the slurry phase polymerization at 85 and 95 °C.

	ka [s^{-1}]	*kp* [lt ($mol\ s^{-1}$)]	*kd* [s^{-1}]
Slurry phase polymerization [85 °C]	$2.5e^{-4}$	195.0	$3.5e^{-4}$
Slurry phase polymerization [95 °C]	$8.0e^{-4}$	110.0	$1.5e^{-4}$

the transfer kinetic parameter via the use of Equation (18). For multi-site type catalysts, a deconvolution step is needed in advance in order to reveal the exact position of the MWD of each site type. The Borealis proprietary software tool BorMol was employed for all deconvolution calculations.[6]

In order to decide on the minimum number of site types to be employed, a deconvolution analysis was performed for all available MWDs coming from slurry phase polymerizations at 85 and 95 °C. All cases shared the same deconvolution trend and indicatively, the effect of the number of site types to the sum of the least squares difference (between the experimentally acquired and the reconstructed MWD) for run 1 is presented in **Figure 6**. Based on this analysis, it was decided to select six site types.

The next deconvolution step refers to the initial site type fraction to be considered. Assuming the same activation, deactivation, and propagation behavior for each site type, this fraction would later correspond to the polymer weight fraction as well. Thus, if the assumption holds true, we should expect that the estimated weight fraction should remain constant for all slurry phase polymerization experiments, at both 85 and 95 °C. Deconvolution analysis for all slurry phase runs was performed for six site types without restricting the weight fraction. The analysis indeed revealed homogeneous results regarding the weight fraction of each site type, confirming the assumption (the fraction results for each site type for all cases studied exhibited a standard deviation value less than 10%). A second optimization procedure was employed in order to estimate the optimum weight fraction for each site type for the minimum deviation from the experimentally

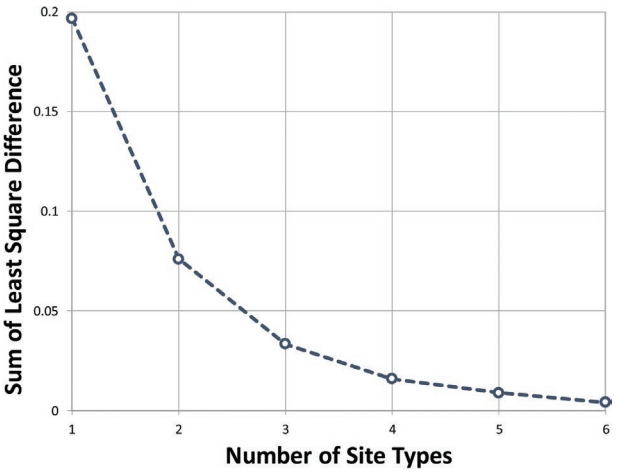

Figure 6. Effect of the number of site types on the sum of the least squares difference between the experimentally acquired and the reconstructed MWD (run 1).

acquired MWDs for all slurry cases. The optimized deconvolution results revealed that the same weight fraction may be employed, exhibiting a standard deviation value less than 0.8% for all cases (comparing the reconstructed to the measured MWD). The estimated weight fraction is presented in **Table 3**. An indicative MWD reconstruction result is depicted in **Figure 7**.

The effect of the hydrogen feed on the number average molecular weight of the deconvoluted site types for all slurry phase polymerization experiments, at both 85 and 95 °C is depicted in **Figure 8**. It is noted that the hydrogen feed takes also into account the hydrogen amount added during the prepolymerization phase since it remained within the reactor during the slurry phase polymerization (for this case, 0.9 g).

Rearranging the information of Figure 8 using Equation (18) and considering the hydrogen concentration instead of the batch feed value (using thermodynamic calculations), we can

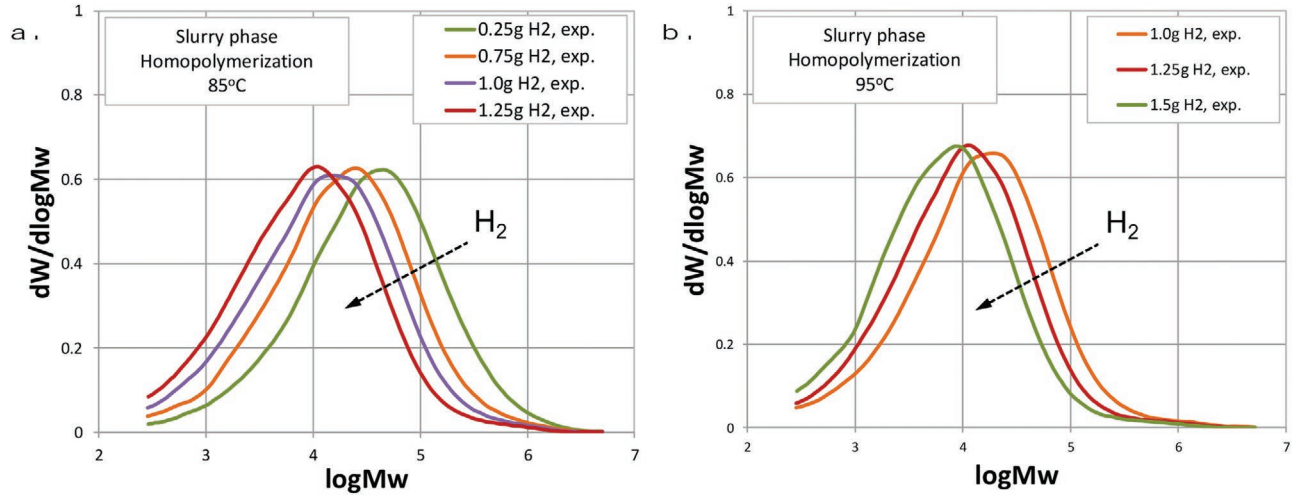

Figure 5. a) Polymer MWD for slurry phase homopolymerization at 85 °C (runs 2–5) and b) 95 °C (runs 7–9).

Table 3. Initial site fraction and corresponding standard deviation values.

	Site type					
	1	2	3	4	5	6
Weight fraction [%]	5.0	16.0	33.0	30.0	13.0	3.0

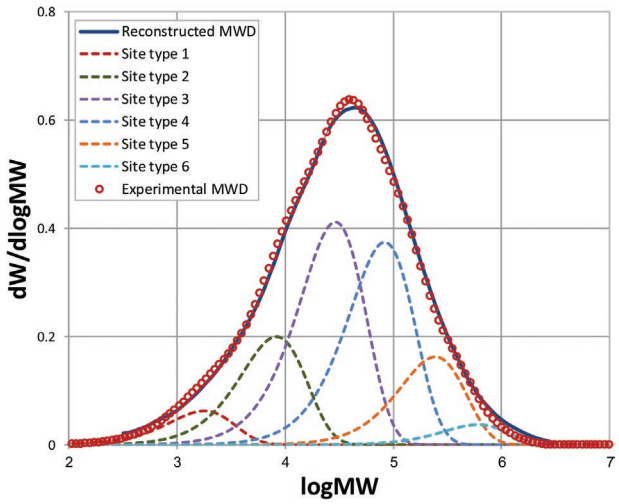

Figure 7. Deconvolution results for six site types (run 1).

reveal the effect of hydrogen concentration on the site type deconvoluted value of the transfer kinetic parameter. Going one step further, for each site type, the kinetic transfer parameter can be split into its components. For this case, we can assume that transfer occurs either spontaneous or due to the use of hydrogen and Equation (19) becomes

$$k_t^i = k_{t,H}^i [H] + \cdots + k_{t,sp}^i \quad (29)$$

In **Figure 9**, the effect of hydrogen concentration on the site type deconvoluted value of the transfer kinetic parameter for the slurry phase homopolymerization at 85 °C as well as the estimation of the kinetic transfer components for the first site type are presented.

4.4. Polymer Reaction Engineering: Multistage Polymerization

The kinetic parameter estimation methodology discussed remains valid for multistage polymerizations. However, an additional split calculation step is required in order to determine the fraction of the "fresh" polymer produced during this phase, since the polymer already includes the fraction produced in earlier polymerization stages.

The first polymerization stage for all multistage runs 10–12 is a copy of run 7. The final MWD and CC along the MWD needs to be split to its slurry and gas phase contribution (Equations (21)–(23)). This split results for run 11 (revealing the "fresh" polymer produced in gas phase) are presented in **Figure 10**. The experimentally measured MWDs and CC along the MWD as well as the split results for Runs 10–12 are presented in **Figure 11**.

The comonomer effect on the activity profile for gas-phase copolymerization at 95 °C, together with the corresponding apparent propagation parameter values for the cases studied are presented in **Figure 12**. Overall, the experimental results followed the theoretically expected behavior: The comonomer addition decreased the polymerization rate since lower amount of monomer is needed to reach the set-point pressure and typical comonomers exhibit lower propagation rates. This effect in turns affects the MWD of the polymer produced, shifting it to lower chain length. In some cases, the comonomer addition may actually lead to increased polymerization rates due to strong co-solubility effects (i.e., the addition of comonomer enables higher amount of monomer to be added in order to reach the same set-point pressure). In this case, the higher monomer concentration value, compared to the case without

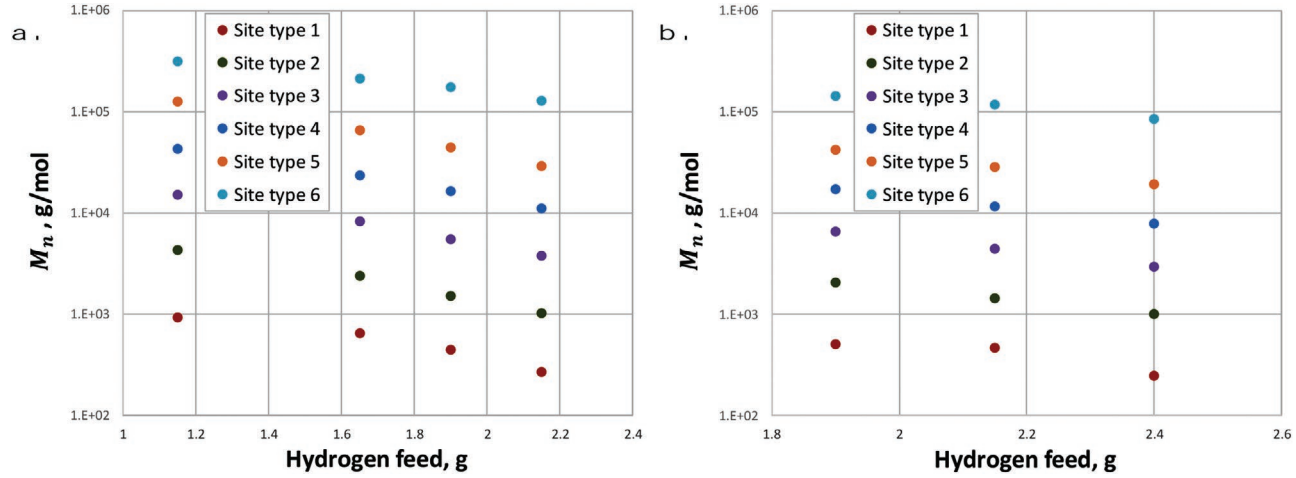

Figure 8. Effect of hydrogen batch feed on the number average molecular weight, M_n, of the deconvoluted site types for slurry phase homopolymerization at a) 85 °C (runs 2–5) and b) at 95 °C (runs 7–8).

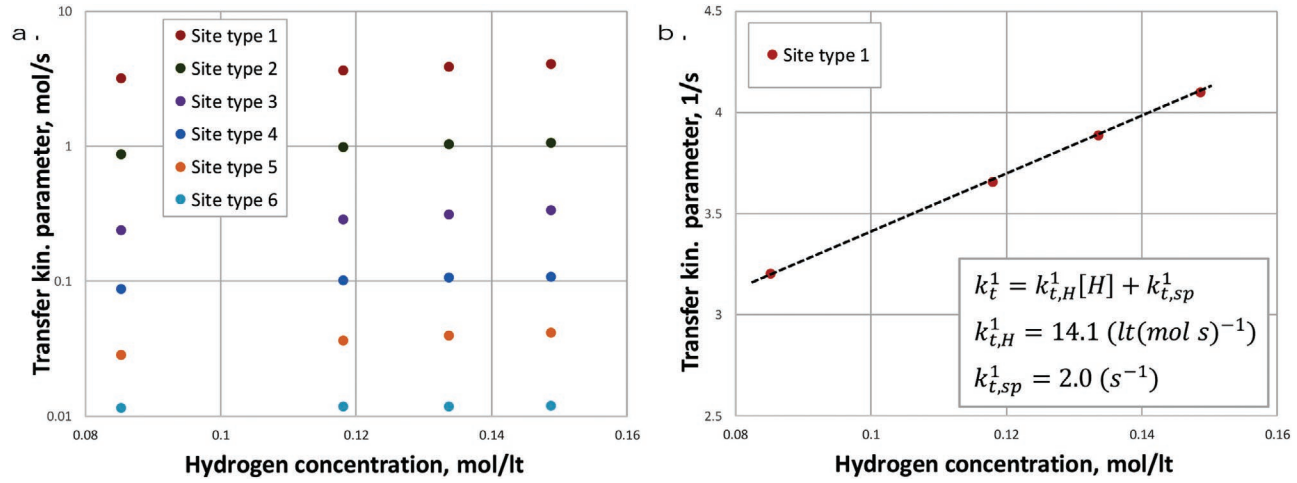

Figure 9. a) Effect of hydrogen concentration on the site type deconvoluted value of the transfer kinetic parameter slurry phase homopolymerization at 85 °C (runs 2–5) and b) estimation of transfer to hydrogen and spontaneous components for the first site type b).

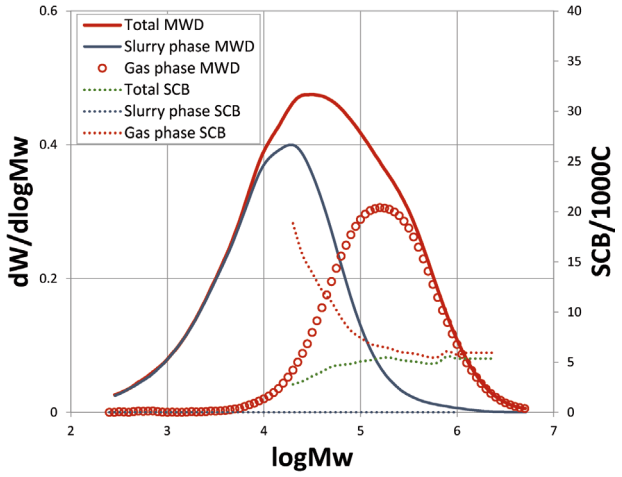

Figure 10. MWD split to slurry and gas phase contribution (run 11).

the comonomer addition, leads to higher polymerization rate. A proper PRE analysis should decouple the thermodynamic from the kinetic effects, providing constant kinetic parameter values.

In order to properly consider the comonomer addition effects, the apparent propagation rate needs to be split to its binary components (Equations (12)–(16)). Initially, the assumption of the same propagation kinetic parameters for all site types can be employed. If this is not enough in order to explain the experimentally acquired activity profile together with the comonomer composition, more complex solutions should be followed. An optimization procedure is then proposed in order to reduce the difference of the reconstructed activity profile and comonomer content (or the CC along the MWD) to the corresponding experimental values. In this analysis, detailed thermodynamic considerations need to be included for capturing the underlying non-linear

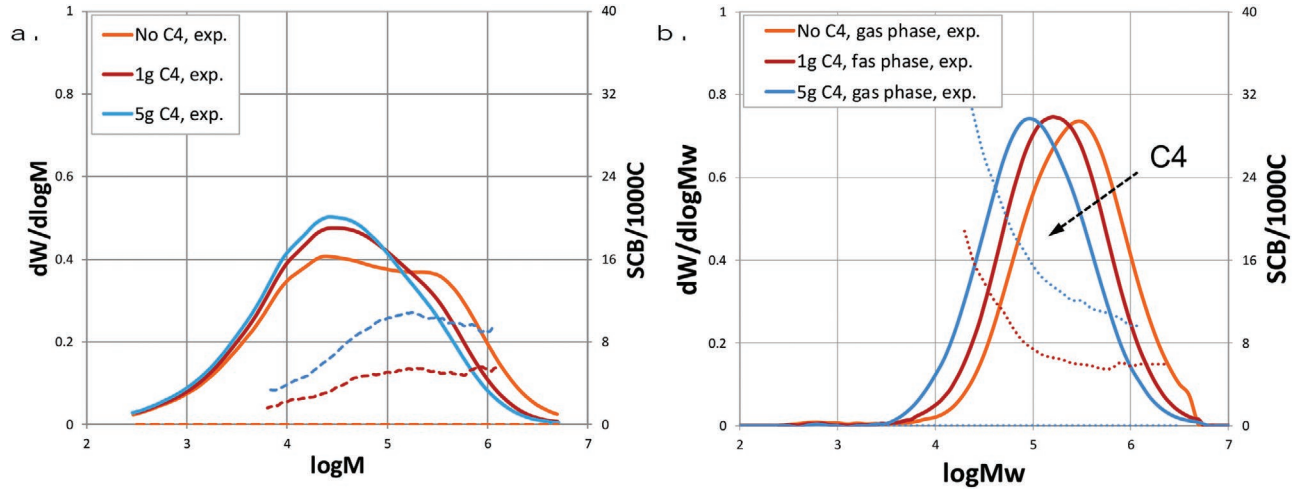

Figure 11. a) Experimentally measured MWD and CC along the MWD and b) gas phase split for multistage copolymerization at 85 °C b) (runs 10–12).

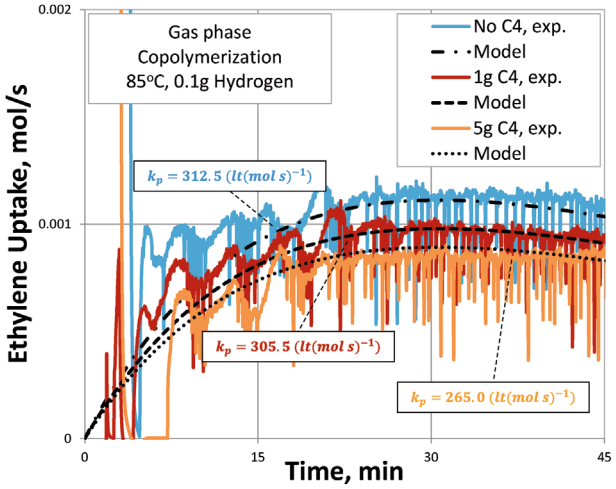

Figure 12. Activity profile for gas-phase copolymerization at 85 °C (runs 10–12).

co-solubility effects. This detailed PRE analysis goes beyond the scope of this work and will not be discussed further in this study.

The PRE methodology can continue, splitting the gas phase MWD to site types' contribution. Following the assumption of the same activation, deactivation, and propagation behavior for each site type, should enable the same site type fraction to further explain the gas phase MWDs. The MWD deconvolution results were then used to attribute the constant comonomer incorporation value (in terms of SCB/1000C) per site type. The deconvolution analysis was performed for runs 10–12 using the exact same site type fraction (Table 3). In all cases, the standard deviation between the measured MWD and the reconstructed one was lower than 0.6% increasing our confidence on the modeling results. Indicatively, the deconvolution results for run 11 are presented in **Figure 13**. This analysis provides us useful insight regarding both the position of the MWD of each site type as

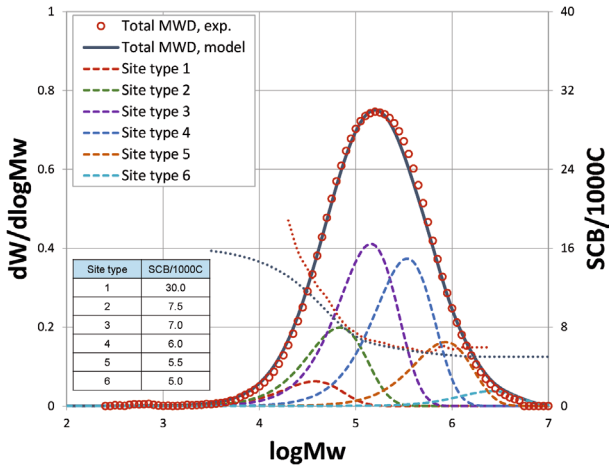

Figure 13. Deconvolution results for six site types (gas phase polymerization at 85 °C, 1g C4) (run 11).

well as its ability for comonomer incorporation. This way, the PRE methodology may continue toward the detailed reactivity ratio analysis. However, this analysis is beyond the scope of this work.

5. Conclusion

The work presented focused on the first modeling step of the PRE pathway, aiming to establish a connection between the polymerization process conditions, polymer microstructure, and end-use properties. An integrated PRE methodology for capturing the reaction performance single- and multi-site type catalysts was proposed and discussed in detail. According to the methodology proposed, the catalyst kinetic parameters are estimated based on a series of targeted bench-scale polymerization experiments and characterization combined with polymer reaction engineering modeling. These kinetic parameters (that should remain constant) describe the catalyst reaction performance and they constitute the cornerstone of the PRE pathway, without which none of the modeling steps can be established. The modeling of the particle size distribution of the polymer produced as well as further connection to first and second level properties (including rheological and mechanical properties) are of great importance and will be the matter of future work of this consortium.

Acknowledgements

The authors acknowledge financial support through the COMET Centre CHASE (project No 868615), which is funded within the framework of COMET – Competence Centers for Excellent Technologies by BMVIT, BMDW, the Federal Provinces of Upper Austria and Vienna. The COMET program is run by the Austrian Research Promotion Agency (FFG).

Conflict of Interest

The authors declare no conflict of interest.

Keywords

kinetics (polym.), microstructure, modeling, polyethylene (PE), Ziegler–Natta polymerization

Received: May 30, 2020
Revised: August 7, 2020
Published online:

[1] W. Kaminsky, *J. Polym. Sci., Part A: Polym. Chem.* **2004**, *42*, 3911.
[2] D. W. Sauter, M. Taoufik, C. Boisson, *Polymers* **2017**, *9*, 185.
[3] J. B. P. Soares, V. Touloupidis, *In Multimodal Polymers with Supported Catalysts: Design and Production* (Ed.: D. Jeremic, F. Prades, A. Albunia), Springer, New York **2019**, p. 115.
[4] V. Touloupidis, C. Wurnitsch, A. Albunia, G. Galgali, *Macromol. Theory Simul.* **2016**, *25*, 392.
[5] M. Ruff, C. Paulik, *Macromol. React. Eng.* **2012**, *6*, 302.
[6] V. Touloupidis, A. Albrecht, J. B. P. Soares, *Macromol. React. Eng.* **2018**, *12*, 1700056.

[7] J. B. P. Soares, T. McKenna, *Polyolefin Reaction Engineering*, Wiley-VCH, Weinheim, Germany **2012**.
[8] V. Touloupides, V. Kanellopoulos, P. Pladis, C. Kiparissides, D. Mignon, P. Van-Grambezen, *Chem. Eng. Sci.* **2010**, *65*, 3208.
[9] V. Touloupidis, *Macromol. React. Eng.* **2014**, *8*, 508.
[10] A. Alshaiban, J. B. P. Soares, *Macromol. React. Eng.* **2012**, *6*, 265.
[11] A. Alshaiban, J. B. P. Soares, *Macromol. React. Eng.* **2014**, *8*, 723.
[12] K. Chen, S. Mehdiabadi, B. Liu, J. B. P. Soares, *Macromol. React. Eng.* **2016**, *10*, 551.
[13] J. B. P. Soares, A. E. Hamielec, *Prog. Polym. Sci.* **1996**, *21*, 651.
[14] J. B. P. Soares, A. E. Hamielec, *Polymer* **1995**, *36*, 2257.
[15] J. B. P. Soares, A. E. Hamielec, *Macromol. Theory Simul.* **1995**, *4*, 305.
[16] S. Anantawaraskul, W. Bongsontia, J. B. P. Soares, *Macromol. React. Eng.* **2011**, *5*, 549.
[17] A. A. Alghyamah, J. B. P. Soares, *Macromol. Rapid Commun.* **2009**, *30*, 384.
[18] M. A. Al-Saleh, J. B. P. Soares, T. A. Duever, *Macromol. React. Eng.* **2010**, *4*, 578.
[19] M. A. Al-Saleh, J. B. P. Soares, T. A. Duever, *Macromol. React. Eng.* **2011**, *5*, 587.
[20] C. Hornchaiya, S. Anantawaraskul, J. B. P. Soares, S. Mehdiabadi, *Macromol. Chem. Phys.* **2019**, *220*, 1800522.